Thermodynamics of Cyclohexanone Oxime

Dzmitry H. Zaitsau, Yauheni U. Paulechka, Gennady J. Kabo,* and Andrey V. Blokhin

Chemistry Faculty, Belarusian State University, Leningradskaya 14, 220030 Minsk, Belarus

Vladimir N. Emel'yanenko, Sergey P. Verevkin, and Andreas Heintz

Department of Physical Chemistry, University of Rostock, Hermannstr. 14, 18051 Rostock, Germany

The heat capacity of cyclohexanone oxime in the interval of (5 to 370) K was measured in an adiabatic calorimeter. The triple-point temperature $T_{fus} = (362.20 \pm 0.04)$ K and the enthalpy of fusion $\Delta_{cr}^{liq}H_m^\circ = (12454 \pm 20)$ J·mol^{-1} were determined. The vapor pressure was measured by the Knudsen method over crystalline cyclohexanone oxime in the interval of (288 to 323) K and by the transpiration method over crystalline, $T =$ (286 to 348) K, and liquid, $T =$ (365 to 395) K, cyclohexanone oxime. Thermodynamic properties in the ideal-gas state were calculated based on the experimental molecular and spectral data and the results of DFT (B3LYP/6-311G(d)) calculations. The experimental and calculated values of the entropy of gaseous cyclohexanone oxime agree within 1 % in the interval of (310 to 362.2) K.

Introduction

Cyclohexanone oxime ($C_6H_{11}NO$), which will be referred by the acronym (CHO) throughout the paper, is an intermediate in the caprolactam synthesis. In industry, isomerization of CHO is carried out with the use of oleum. This gives rise to technical and ecological problems related with utilization of sulfuric acid or its derivatives remaining after caprolactam separation. Nowadays, alternative schemes of the synthesis are being developed, e.g., with the use of ionic liquids.[1]

The thermodynamic properties for CHO in the condensed and gaseous states were reported earlier.[2] It was noted that the difference in the sublimation enthalpies obtained from the Knudsen method and by calorimetry was 2.5 kJ·mol^{-1} which is double the value of the combined uncertainty of both the methods. Afterward,[3] it was shown that the isotropy failure of a gas in an effusion cell should be taken into account to obtain the reliable vapor pressure and the vaporization enthalpy from the Knudsen experiments. The heat capacity values from ref 2 also do not seem to be reliable enough. For example, the heat capacity for CHO[2] was 1.5 J·K^{-1}·mol^{-1} at 5 K. This value is much higher than the heat capacity of crystalline caprolactam at the same temperature.[4] There was a peak in the heat capacity curve at $T = 273$ K probably caused by the presence of water in the sample.[2]

The above-mentioned reasoning together with the development of the new computational methods has brought us to a conclusion that a new comprehensive study of thermodynamic properties for CHO was necessary. The results of the study are reported in this work, and they include heat capacity and parameters of phase transitions from adiabatic calorimetry, vapor pressures over crystalline and liquid CHO, and thermodynamic properties of CHO in the ideal-gas state obtained from the statistical thermodynamic and quantum chemical calculations.

* To whom correspondence should be addressed. Tel./fax: +375-17-2203916. E-mail: kabo@bsu.by.

Experimental

Sample. The commercial sample of CHO (Grodno Azot) with the initial mass fraction purity of 0.95 (water was the main impurity) was sublimed at $T = 338$ K and $p = 0.3$ kPa. Additionally, it was dried over P_2O_5 for 2 weeks. The mass fraction of CHO in the sample was found to be 0.9997 ± 0.0003 with a CHROM-5 chromatograph equipped with a katharometer as a detector. A column (Polysorb stationary phase) of 1 m length and 3 mm diameter was used. The temperature of the column during analysis was $T = 473$ K. From the fractional melting experiments in an adiabatic calorimeter, the mole fraction purity of the sample was 0.9998 ± 0.0001. This sample was used in the calorimetric and effusion experiments.

For the transpiration experiments, the commercially available CHO (Merck, mass fraction 0.98) was freshly sublimed prior to experiment. The degree of purity was determined using a Hewlett-Packard gas chromatograph 5890 Series II equipped with a flame ionization detector and a Hewlett-Packard 3390A integrator. A capillary column HP-5 (stationary phase cross-linked 5 % PH ME silicone) was used with a column length of 30 m, an inside diameter of 0.32 mm, and a film thickness of 0.25 μm. The standard temperature program of the GC was $T = 353$ K for 60 s followed by a heating rate of 10 K·min^{-1} to $T = 523$ K. No impurities (mass fraction greater than 0.0002) could be detected in the sample used for the transpiration measurements.

Adiabatic Calorimetry. The heat capacity of CHO under saturated vapor pressure (C_s) in the interval of (5 to 370) K and the fusion enthalpy were determined in a Termis TAU - 10 adiabatic calorimeter. The apparatus and experimental procedures were described elsewhere.[5] The sample was loaded in the calorimetric container in a drybox. The uncertainty of the heat capacity measurements was ± 0.4 % in the interval of (20 to 370) K and 1 % in the range of (10 to 20) K and did not exceed 2 % below 10 K.[5]

Spectrometry. The IR spectra for CHO in a CCl_4 solution and in KBr pellets were recorded with a Bruker Vertex 70

10.1021/je700546r CCC: $40.75
Published on Web 02/16/2008

Table 1. Experimental Heat Capacities for CHO (M = 0.113159 kg·mol^{-1})

T / K	C_s^a / J·K^{-1}·mol^{-1}	T / K	C_s^a / J·K^{-1}·mol^{-1}	T / K	C_s^a / J·K^{-1}·mol^{-1}	T / K	C_s^a / J·K^{-1}·mol^{-1}
Series 1		214.38	126.63	310.43	193.00	121.72	75.080
Crystal		216.30	128.63	312.22	193.77	123.73	75.978
79.94	56.264	218.21	130.69	314.11	194.56	125.75	76.855
81.67	57.037	220.14	132.72	316.00	195.45	127.76	77.722
83.39	57.845	222.06	134.69	317.89	196.42	129.79	78.601
85.10	58.585	224.01	136.62	319.77	197.45	131.81	79.494
86.83	59.395	225.92	138.42	Series 3		133.83	80.384
88.55	60.203	227.85	140.09	Crystal		135.86	81.282
90.28	61.007	229.78	141.60	305.83	191.51	137.88	82.162
92.01	61.805	231.71	143.03	307.60	191.89	139.90	83.046
93.75	62.621	233.64	144.32	309.38	192.47	141.92	83.955
95.49	63.419	235.57	145.51	311.16	193.22	143.95	84.852
97.23	64.210	237.50	146.68	312.94	194.04	145.97	85.734
98.97	65.031	239.43	148.81	314.72	194.70	148.00	86.671
100.72	65.829	241.36	153.60	316.49	195.61	150.03	87.591
102.52	66.597	243.30	148.43	318.27	196.48	152.05	88.519
104.37	67.436	245.25	149.53	320.04	197.43	154.08	89.422
106.23	68.291	247.18	150.98	321.81	198.43	156.10	90.343
108.09	69.080	Series 2		323.58	199.58	158.12	91.274
109.95	69.916	Crystal		325.35	200.52	160.13	92.237
111.81	70.758	217.00	129.41	327.11	201.48	162.15	93.182
113.68	71.569	218.98	131.50	328.87	202.64	164.16	94.145
115.55	72.371	220.87	133.52	330.63	203.71	166.17	95.080
117.41	73.203	222.75	135.43	332.40	204.63	168.18	96.066
119.29	74.027	224.62	137.24	334.15	205.60	170.18	97.045
121.16	74.846	226.48	138.92	335.91	206.77	172.19	98.050
123.03	75.633	228.33	140.45	337.67	207.80	174.19	99.046
124.91	76.462	230.18	141.86	339.42	208.77	176.19	100.08
126.79	77.293	232.03	143.15	341.17	209.83	178.20	101.13
128.67	78.113	233.87	144.33	342.93	210.86	180.20	102.17
130.55	78.910	235.71	145.65	344.68	212.10	182.19	103.23
132.43	79.754	237.54	146.94	346.43	213.18	184.18	104.31
134.31	80.585	237.54	146.94	348.18	214.14	186.16	105.44
136.20	81.418	239.36	148.90	349.93	215.30	188.14	106.57
138.09	82.254	241.18	153.75	351.67	216.38	190.12	107.71
139.98	83.084	242.99	148.41	353.42	217.49	192.10	108.92
141.87	83.927	244.82	149.34	355.16	218.64	194.08	110.15
143.76	84.770	246.66	150.69	Melt		196.05	111.36
145.65	85.617	248.48	152.19	356.90	220.12	198.02	112.60
147.54	86.492	250.29	153.82	358.64	222.02	199.97	113.87
149.44	87.350	252.11	155.49	360.36	229.30	202.00	115.31
151.34	88.171	253.91	157.22	361.67	646.2	203.92	116.79
153.24	89.045	255.71	159.00	Liquid		205.74	118.31
155.13	89.889	257.50	160.82	364.59	273.00	207.56	119.91
157.03	90.765	259.28	162.64	366.16	273.91	209.36	121.66
158.93	91.646	261.05	164.53	367.73	274.96	211.17	123.38
160.83	92.535	262.82	166.41	Series 4		212.97	125.27
162.73	93.455	264.58	168.33	Liquid		214.76	127.11
164.63	94.346	266.34	170.21	363.80	272.42	216.54	128.94
166.54	95.254	268.08	172.13	365.34	273.22	218.32	130.87
168.44	96.201	269.82	174.08	366.88	274.16	220.09	132.70
170.35	97.126	271.56	175.95	368.42	275.12	Series 6	
172.26	98.073	273.28	177.73	Series 5		Crystal	
174.17	99.058	275.02	179.53	Crystal		217.73	130.26
176.08	100.02	276.74	181.37	82.20	57.238	219.50	132.12
177.99	101.03	278.45	183.01	84.24	58.198	221.26	133.99
179.90	102.04	280.15	184.62	86.15	59.049	223.02	135.78
181.81	103.07	281.85	186.12	88.07	59.960	224.76	137.52
183.72	104.11	283.54	187.50	90.00	60.852	226.50	139.12
185.64	105.14	285.24	188.79	91.95	61.754	228.24	140.60
187.55	106.25	286.93	189.90	93.89	62.671	229.98	141.91
189.46	107.37	288.61	190.97	95.85	63.556	231.71	143.15
191.37	108.48	290.29	191.83	97.81	64.447	233.43	144.26
193.29	109.62	291.97	192.78	99.77	65.369	235.14	145.41
195.20	110.84	293.65	193.64	101.74	66.248	236.85	146.62
197.13	112.05	295.32	194.51	103.72	67.142	238.56	147.84
199.05	113.28	297.00	195.34	105.70	68.037	239.79	150.04
200.97	114.62	298.66	196.34	107.69	68.921	241.48	154.07
202.89	116.00	300.33	197.85	109.68	69.811	243.42	148.52
204.81	117.51	301.99	196.75	111.68	70.687	245.37	149.83
206.72	119.13	303.67	191.89	113.68	71.558	247.07	151.16
208.63	120.93	305.36	191.49	115.69	72.449	248.78	152.63
210.55	122.71	307.05	191.78	117.70	73.346	250.48	154.01
212.46	124.68	308.74	192.41	119.71	74.215	252.36	155.81

Table 1 Continued

T/K	C_s^a/J·K^{-1}·mol^{-1}	T/K	C_s^a/J·K^{-1}·mol^{-1}	T/K	C_s^a/J·K^{-1}·mol^{-1}	T/K	C_s^a/J·K^{-1}·mol^{-1}
254.12	157.42	331.06	203.58	334.74	205.77	14.03	6.5715
255.80	159.11	332.88	204.71	336.49	206.75	14.64	7.1526
257.47	160.79	334.70	205.74	338.25	207.78	15.26	7.7959
259.14	162.49	336.52	206.77	339.99	208.85	15.98	8.6012
260.80	164.29	338.35	207.86	341.74	209.95	16.81	9.4967
262.46	166.09	340.17	209.00	343.49	210.94	17.65	10.365
264.11	167.84	341.99	210.15	345.25	212.02	18.49	11.280
265.75	169.58	343.81	211.29	346.99	213.12	19.34	12.181
267.39	171.43	345.63	212.36	348.74	214.13	20.19	13.084
269.02	173.27	347.45	213.43	350.48	215.24	21.32	14.349
270.64	175.04	349.27	214.58		Melt	22.74	15.894
272.26	176.79	351.09	215.74	352.41	216.96	24.16	17.456
273.87	178.52	352.91	217.26	354.55	219.52	25.59	18.999
275.47	180.26	354.73	219.00	356.67	222.61	27.02	20.499
277.08	181.92	356.54	221.91	358.75	231.68	28.49	21.997
278.67	183.43	358.35	227.53	360.64	314.35	30.12	23.630
280.26	185.03		Liquid	361.76	1583.1	31.73	25.216
281.85	186.38	367.52	274.57		Liquid	33.50	26.876
283.43	187.69	368.96	275.31	364.48	272.66	35.28	28.484
285.01	188.93		Series 7	365.92	273.48	37.06	30.012
286.58	189.97		Crystal	367.36	274.33	38.84	31.474
288.15	191.00	292.14	192.79	368.79	275.25	40.63	32.894
289.72	191.92	293.70	193.66		Series 8	42.51	34.381
291.28	192.69	295.26	194.41		Crystal	44.49	35.899
292.85	193.59	296.81	195.24	4.900	0.33898	46.48	37.344
294.41	194.19	298.36	196.04	5.136	0.39671	48.47	38.758
295.97	194.99	299.91	197.34	5.378	0.46488	50.46	40.107
297.53	195.76	301.45	198.75	5.624	0.54188	52.45	41.416
299.09	196.66	303.01	192.59	5.878	0.62777	54.45	42.643
300.64	198.30	304.57	191.66	6.165	0.73332	56.45	43.840
302.19	195.88	306.14	191.69	6.485	0.86213	58.46	45.024
303.76	191.84	307.71	191.96	6.812	1.0064	60.47	46.162
305.34	191.58	309.27	192.53	7.147	1.1673	62.48	47.276
306.91	191.81	310.95	193.22	7.488	1.3381	64.50	48.369
308.49	192.20	312.72	193.93	7.836	1.5301	66.51	49.443
310.07	192.72	314.48	194.70	8.187	1.7352	68.52	50.507
311.68	193.28	316.25	195.55	8.542	1.9562	70.54	51.546
313.36	194.05	318.01	196.38	8.902	2.1896	72.56	52.586
315.03	194.86	319.77	197.36	9.268	2.4377	74.59	53.590
316.71	195.66	321.54	198.27	9.636	2.7078	76.61	54.603
318.38	196.46	323.30	199.26	10.00	2.9809	78.65	55.597
320.11	197.40	325.05	200.28	10.48	3.3609	80.68	56.576
321.98	198.37	326.81	201.27	11.06	3.8301	82.71	57.543
323.80	199.44	328.56	202.22	11.64	4.3255	84.75	58.471
325.62	200.47	330.32	203.27	12.23	4.8537		
327.43	201.55	331.23	203.73	12.83	5.4079		
329.24	202.56	332.98	204.75	13.43	5.9918		

[a] Average heat capacity at the mean temperature of an experiment.

spectrometer in a wavenumber range of (4000 to 400) cm^{-1} with resolution of 2 cm^{-1}.

Knudsen Method. The vapor pressure (p^{sat}) for CHO in the interval of (291 to 323) K was measured by the integral Knudsen method. The apparatus and the experimental technique were described elsewhere.[3] The combined uncertainty of the measurements was established to be ± 5 %.

Three nickel membranes were used in the effusion experiments: membrane 1 with thickness $l = (50 \pm 1)$ μm and diameter $d = (0.1833 \pm 0.0004)$ mm, membrane 2 with $l = (84 \pm 1)$ μm and $d = (0.4467 \pm 0.0005)$ mm, and membrane 3 with $l = (50 \pm 1)$ μm and $d = (0.8370 \pm 0.0005)$ mm.

The vapor pressures were calculated according to the equation[4]

$$p^{sat} = \left(\frac{1}{\alpha\gamma S_{samp}} + \frac{1}{k_W S_{orif}}\right)\frac{\Delta m}{\tau}\sqrt{\frac{2\pi RT}{M}} \qquad (1)$$

where p^{sat} is the vapor pressure for CHO; Δm is the mass loss during the vacuum exposure time τ; S_{orif} is the cross sectional area of the orifice; T is the temperature of the heat carrier in the thermostat where the copper block with an effusion cell is placed; M is the vapor molar mass ($M = 113.16$ g·mol^{-1} was assumed);[6] S_{samp} is the exposed sample surface; $R = 8.31447$ J·K^{-1}·mol^{-1}; and $\alpha\gamma$ is the product of the condensation coefficient (Langmuir) and the roughness coefficient for the sample surface.

The k_W transmission coefficient was determined according to Wahlbeck's theory of isotropy failure of a gas in the Knudsen cell.[7] The calculation technique was described earlier.[3] The effective diameter for the CHO molecule ($\sigma = 0.578$ nm) was calculated from its excluded volume[8] assuming the molecule to be spherical. The excluded volume was calculated in the Tinker 4.0 package[8] using the molecular geometry obtained in the quantum chemical calculations and the van der Vaals radii from ref 9.

The k_W coefficient depends on the vapor pressure in the effusion cell and the Knudsen number. The vapor pressure in the effusion cell can deviate from the equilibrium value due to

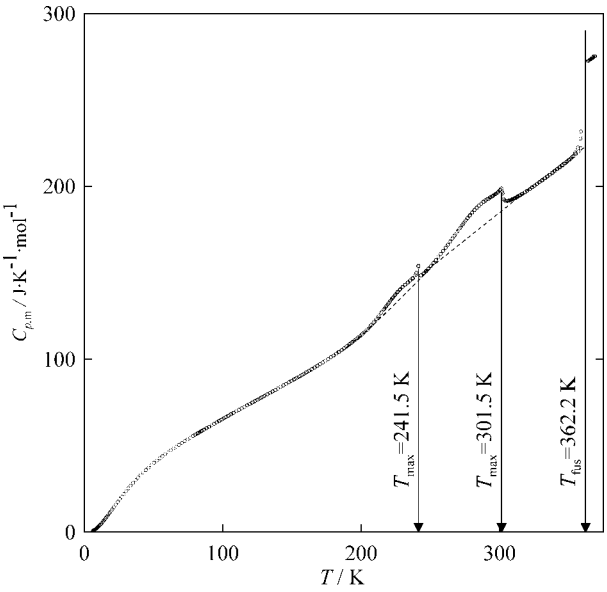

Figure 1. Temperature dependence of the heat capacity for cyclohexanone oxime. The broken curve shows the baseline used to calculate the thermodynamic properties for the anomalies.

Table 2. Comparison of the Thermodynamic Properties Obtained in the Previous Study[2] and This Work

	$\Delta_0^T S_m^\circ$ (298.15K)	$\Delta_0^T S_m^\circ$ (g, 320 K)		$C_{p,m}^\circ$ (g, calc)	
	J·K^{-1}·mol^{-1}	J·K^{-1}·mol^{-1}		J·K^{-1}·mol^{-1}	
origin	J·K^{-1}·mol^{-1}	exptl	calcd	298 K	500 K
ref 2	185.1 ± 0.5	371.5 ± 1.0	379.22	137.0	217.8
this work	185.8 ± 0.8	373.5 ± 1.6	370.6	135.7	228.7

a high effusion flow through the orifice or $\alpha\gamma << 1$ for crystals.[10] To get the equilibrium vapor pressure values, a few membranes were used in the experiments. The $\alpha\gamma$ value was found from minimization of the $\sum_i (\ln(p_i^{sat}(\alpha\gamma, T)/p_i^{sat}(\text{calcd})))^2$ function. Here p_i^{sat}(calcd) is the vapor pressure calculated from the Clarke equation[11] (see below).

In many cases, the corrections for isotropy failure and undersaturation counterbalance each other. Therefore, the neglect of these two corrections may give the results close to those from the other methods.

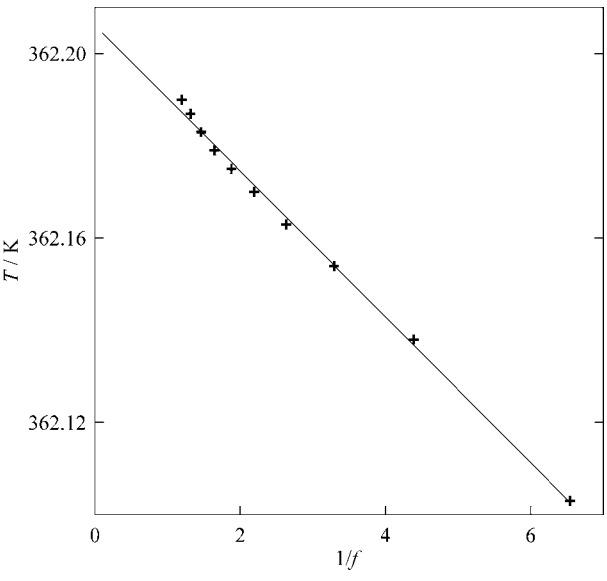

Figure 2. Temperature of the melting system vs inverse melted fraction.

Table 3. Determination of the Molar Enthalpy of Fusion for CHO

T_{start}	T_{end}	Q	$\Delta_{cr}^{liq} H_m^0$
K	K	J·mol^{-1}	J·mol^{-1}
354.41	363.44	14516	12461[a]
350.75	365.41	15851	12464
349.77	364.46	15780	12442[a]
350.41	364.23	15607	12469
348.93	363.06	15573	12436
average			(12454 ± 20)

[a] From the fractional melting experiments.

Table 4. Thermodynamic Properties of CHO in the Condensed State

T	$C_{p,m}^\circ$	$\Delta_0^T H_m^\circ/T$	$\Delta_0^T S_m^\circ$	$-\Delta_0^T G_m^\circ/T$
K	J·K^{-1}·mol^{-1}	J·K^{-1}·mol^{-1}	J·K^{-1}·mol^{-1}	J·K^{-1}·mol^{-1}
		Crystal		
5	0.3674	0.09088	0.1211	0.03019
10	2.982	0.7729	1.027	0.25426
15	7.554	2.233	3.054	0.8213
20	12.90	4.228	5.956	1.728
25	18.36	6.508	9.421	2.912
30	23.53	8.921	13.23	4.311
35	28.21	11.35	17.22	5.869
40	32.42	13.72	21.26	7.540
45	36.26	16.02	25.31	9.290
50	39.78	18.22	29.31	11.09
60	45.91	22.34	37.13	14.78
70	51.28	26.10	44.61	18.51
80	56.24	29.56	51.79	22.23
90	60.87	32.78	58.68	25.90
100	65.47	35.82	65.33	29.51
110	69.94	38.72	71.78	33.06
120	74.33	41.51	78.06	36.55
130	78.70	44.20	84.18	39.98
140	83.10	46.82	90.17	43.35
150	87.59	49.39	96.06	46.67
160	92.16	51.92	101.9	49.94
170	96.94	54.42	107.6	53.16
180	102.1	56.93	113.3	56.34
190	107.7	59.45	118.9	59.49
200	113.9	62.01	124.6	62.60
210	122.3	64.67	130.4	65.69
220	132.6	67.52	136.3	68.76
230	141.9	70.56	142.4	71.83
240	150.7	73.68	148.6	74.90
250	153.4	76.77	154.7	77.97
260	163.4	79.91	160.9	81.04
270	174.5	83.21	167.3	84.12
280	184.4	86.65	173.9	87.21
290	191.9	90.15	180.5	90.31
298.15	196.2	93.00	185.8	92.85
300	197.1	93.64	187.1	93.43
310	192.8	96.51	193.1	96.55
320	197.5	99.59	199.3	99.66
330	203.0	102.6	205.4	102.8
340	209.0	105.7	211.6	105.9
350	215.2	108.7	217.7	109.0
360	221.1	111.8	223.9	112.1
362.20	222.4	112.4	225.2	112.8
		Liquid		
362.20	271.5	146.8	259.6	112.8
365	273.1	147.8	261.7	113.9
370	276.0	149.5	265.4	115.9

Transpiration Method. Vapor pressures were also determined using the method of transference in a stream of nitrogen. The method has been described in detail before[12,13] and has proven to give results in agreement with other established techniques. The temperature dependence of the vapor pressures was used to determine the enthalpies of vaporization of the pure substances. A sample of approximately 0.5 g was mixed with glass beads and placed in a thermostatted U-tube of length 10 cm and diameter 0.5

Table 5. Vapor Pressures of Crystalline CHO by the Knudsen Method ($\sigma = 5.78 \cdot 10^{-10}$ m, $\alpha\gamma = 0.0059$, $S_{sample} = 3.93 \cdot 10^{-4}$ m^2)

T	τ	$10^6\Delta m$	$d_{orifice}$			p^{sat}
K	s	kg	mm	k_W[a]	Kn[b]	Pa
303.74	15420	4.68	0.1833	0.8454	3.02	5.145
308.70	14400	7.26	0.1833	0.8705	1.89	8.370
313.62	7440	6.34	0.1833	0.9030	1.17	13.75
323.32	7200	15.93	0.1833	0.9712	0.49	33.73
323.35	3610	8.24	0.1833	0.9734	0.48	34.72
293.82	11400	7.65	0.4467	0.8997	3.49	1.860
298.77	5445	6.25	0.4467	0.9273	2.12	3.118
303.73	3620	7.17	0.4467	0.9635	1.29	5.234
288.11	7200	9.07	0.8370	1.007	3.86	1.028
293.87	3600	7.89	0.8370	1.041	2.31	1.759

[a] The transmission probability factor was calculated according to Wahlbeck's theory.[3] [b] Kn is the Knudsen number, the ratio of the mean free path and the orifice diameter.

Table 6. Results from Measurements of the Vapor Pressure p of CHO Using the Transpiration Method

T/K[a]	m/mg[b]	$V(N_2)$/dm^3[c]	p^{sat}/Pa[d]
Cyclohexanone Oxime (Sublimation)			
285.7	1.15	32.72	0.78
290.0	0.49	9.22	1.18
292.6	0.76	10.60	1.57
295.1	0.77	7.85	2.15
298.1	0.79	6.19	2.75
298.2	0.76	5.51	3.02
298.2	0.89	6.64	2.93
301.1	0.92	5.13	3.96
302.9	0.89	3.85	5.00
305.4	0.83	2.92	6.26
307.6	1.57	4.28	8.06
310.2	0.80	1.71	10.34
313.0	1.55	2.50	13.60
315.3	0.81	1.10	16.01
318.0	1.50	1.53	21.55
320.3	1.74	1.42	26.71
323.1	1.75	1.14	33.64
325.4	2.25	1.15	42.73
328.0	1.80	0.743	53.12
330.4	3.07	1.01	65.93
333.1	2.80	0.746	82.34
338.2	1.31	0.233	123.2
340.2	1.60	0.253	137.6
343.3	1.86	0.233	175.8
345.6	2.48	0.253	213.0
348.3	2.79	0.233	263.9
Cyclohexanone Oxime (Vaporization)			
364.6	11.17	0.286	862.4
367.9	12.84	0.277	1030.4
370.5	14.82	0.277	1180.9
373.6	17.42	0.277	1388.3
376.6	20.84	0.277	1660.8
377.7	21.92	0.277	1758.7
379.7	24.11	0.277	1921.7
382.8	27.83	0.277	2221.5
385.8	32.23	0.277	2574.1
388.9	38.03	0.277	3046.4
391.9	43.51	0.277	3485.6
394.9	49.66	0.277	3978.3
365.7	9.47	0.233	894.8
369.7	11.84	0.233	1119.1
373.7	14.81	0.233	1405.2
377.8	18.83	0.233	1786.2
381.8	22.49	0.233	2124.3

[a] Temperature of saturation. [b] Mass of transferred sample, condensed at $T = 273$ K. [c] Volume of nitrogen, used to transfer mass m of sample. [d] Vapor pressure at temperature T, calculated from m, and the residual vapor pressure at the cooling temperature $T = 273$ K.

cm. A preheated nitrogen stream was passed through the U-tube at constant temperature (± 0.1 K). The flow rate of the nitrogen stream was measured using a soap film bubble flow meter (± (0.2 to 0.3) %) and optimized to reach the saturation equilibrium of the transporting gas at each temperature under study. We tested our apparatus at different flow rates of the carrier gas to check the lower boundary of the flow, below which the contribution of the vapor condensed in the trap by diffusion becomes comparable to the transpired one. In our apparatus, the contribution due to diffusion was negligible at flow rates down to 0.5 dm$^3 \cdot$h^{-1}. The upper limit for our apparatus was a flow rate of 10.5 dm$^3 \cdot$h^{-1}. Thus, we carried out the experiments using flow rates ranging from (1.2 to 7.2) dm$^3 \cdot$h^{-1} which ensured that transporting gas was in saturated equilibrium with the coexisting solid phase in the saturation tube. The material transported was condensed in a cold trap. The amount of condensed product was determined by GLC analysis using an external standard (hydrocarbon).

The saturation vapor pressure p_i^{sat} at each temperature T_i was calculated from the amount of product collected within a definite period of time, and the small value of the residual vapor pressure at the temperature of condensation was added. Assuming that Dalton's law of partial pressures when applied to the nitrogen stream saturated with the substance is valid, values of p_i^{sat} were calculated

$$p_i = m_i \cdot R \cdot T_a / V \cdot M_i;\ V = V_{N2} + V_i;\ (V_{N2} \gg V_i) \qquad (2)$$

where $R = 8.31447$ J$\cdot$K$^{-1}\cdot$mol^{-1}; m_i is the mass of the transported compound; M_i is the molar mass of the compound; and V_i is its volume contribution to the gaseous phase. V_{N2} is the volume of transporting gas, and T_a is the temperature of the soap film bubble flow meter. The volume of transporting gas V_{N2} was determined from the flow rate and time measurements.

The vapor pressure of CHO was studied above and below the melting point. First, measurements were performed above the liquid sample in the temperature range of (366 to 382) K. Afterward, the sample was cooled below the melting point, and the study of the sublimation pressures using 5° steps down to 298 K was performed. At 298 K, we proved the saturation of the nitrogen stream by measuring vapor pressures at (3.9, 5.6, and 7.2) dm$^3 \cdot$h^{-1}. It is well-known that CHO is a very reactive compound. Hence, we put forth efforts to detect any possible changes in the purity of the sample during its study. The first part of the experiment took about 48 h of continual exposure of the sample to the temperature impact. To check whether any changes occur with the sample due to thermal stress, we reloaded a new portion of the sample into the saturation tube and repeated the measurements of the vapor pressure over the solid sample: the vapor pressures were indistinguishable for both series of measurements. In addition, we controlled the purity of the samples in the saturation tube after completion of experiments, and no changes occurred according to the GC analysis.

Results

Heat Capacity. The experimental heat capacities for CHO in the interval of (5 to 370) K are listed in Table 1 and shown in Figure 1. Two transitions at $T =$ (205 to 246) K and (250 to 305) K were found in the heat capacity curve for the crystalline CHO. The nature of these anomalies in heat capacity was not studied. However, our investigation revealed the reversibility of the observed transitions. Therefore, the entropies of the anomalies were calculated by integrating the ratio of the "excess" heat capacity to the temperature in the interval of

Table 7. Parameters of Clarke and Glew Equations for the Temperature Dependence of Both Crystalline and Liquid–Vapor Pressures of CHO ($p^\circ = 10^5$Pa)

method (phase)	θ/K	A/K	B/K	C	D/K^{-1}	temp. range
Experimental Data Treatment						
[a]Knudsen (cr)	310	-2863 ± 8	9362 ± 183	-6.014	−	(288 to 323) K
[b]transpiration (cr)		-2847 ± 4	9392 ± 66	-6.014	−	(285 to 348) K
[c]Vapor Pressure Data Regression Parameters						
crystal	316	-2731.4 ± 0.4	9377 ± 6	-6.014	−	(285 to 362.2) K
liquid	400	-1170.7 ± 0.6	7402 ± 3	-8.46 ± 0.3	-0.17 ± 0.02	(362.2 to 446) K

[a] Data from Table 4 were used. [b] Data from Table 5 (sublimation) were used. [c] Vapor pressure data from Tables 4 and 5 and ref 15, fusion enthalpy from Table 3, and vaporization enthalpy from ref 2 were used in the regression.

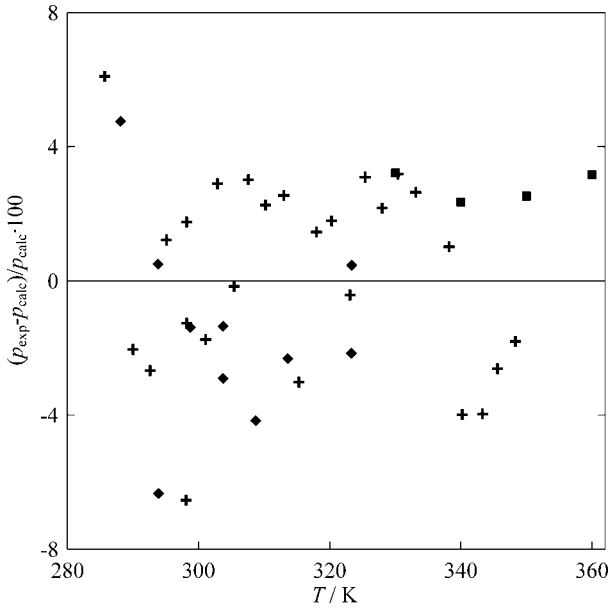

Figure 3. Deviation of the experimental vapor pressure data for crystalline cyclohexanone oxime from the values predicted by eq 3 and Table 7: +, transpiration method data; ♦, effusion method data; ■, data from ref 15.

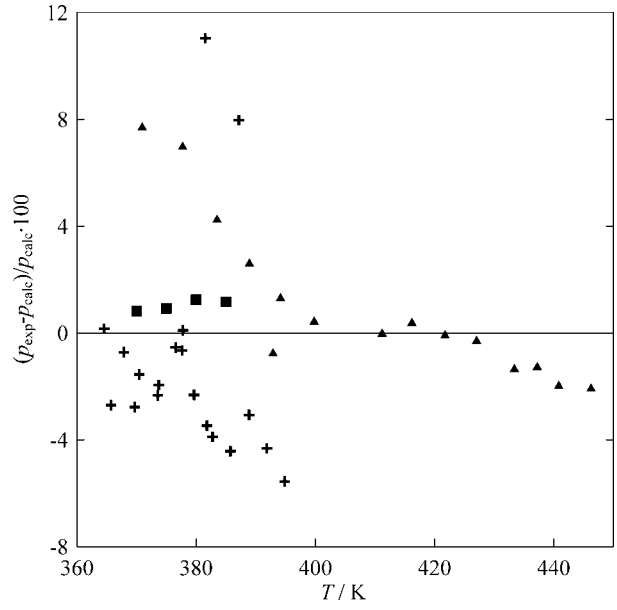

Figure 4. Deviation of the experimental vapor pressure data for liquid cyclohexanone oxime from the values predicted by eq 4 and Table 7: +, transpiration method data; ▲, static method data (previous investigation);[2] ■, data from reference 15.

the anomalies. The temperatures of the maxima in the heat capacity curve are shown in Figure 1.

Thermodynamic parameters of the transitions are: $\Delta_{trs}H_m^\circ$(crIII → crII) = 116 ± 27 J·mol^{-1}, $\Delta_{trs}S_m^\circ$(crIII → crII) = 0.5 ± 0.1 J·K^{-1}·mol^{-1}, $\Delta_{trs}H_m^\circ$(crII → crI) = 403 ± 61 J·mol^{-1}, and $\Delta_{trs}S_m^\circ$(crII → crI) = 1.5 ± 0.2 J·K^{-1}·mol^{-1}.

The high purity of the sample (mole fraction purity of 0.9998) allows us to assert that these transitions are not connected with the presence of cyclohexanol and cyclohexanone in the sample.

Comparing the heat capacity values from the previous investigation[2] and the result of this work, one can see that the difference in heat capacity at 5 K is 1.1 J·K^{-1}·mol^{-1}. For the interval (35 to 100) K, the deviation does not exceed 2.5 %. The previous results obtained in the temperature range (100 to 320) K agree with the results of this work within 1 %, but there was a peak at 273 K in the earlier work.[2] It is likely due to the presence of water in the sample during the previous investigation. The deviation in the heat capacity in the whole temperature range of the investigation exceeds the uncertainty of the used method. Nevertheless, the standard entropy of crystalline CHO changed insignificantly compared with the previous work (Table 2).

Fusion. While cooling the sample from 370 K, the spontaneous crystallization of the supercooled liquid began at T = (354 to 355) K. The sample was kept at T = (362.1 to 362.2) K until the heat evolution had stopped. It took (3 to 4) h. Then, the sample was slowly cooled to 250 K at a cooling rate of (1 to 2) mK·s^{-1}. The crystal obtained this way was used in the fusion enthalpy determination.

The triple-point temperature for CHO, T_{fus} = (362.20 ± 0.04) K, was determined by the fractional melting method (Figure 2). The fusion enthalpy, $\Delta_{cr}^{liq}H_m^\circ$(362.20 K) = (12454 ± 20) J·mol^{-1}, was determined from several experiments (Table 3). The following equation was used to calculate $\Delta_{cr}^{liq}H_m^\circ$:

$$\Delta_{cr}^{liq}H_m = Q - \int_{T_{start}}^{T_{fus}} C_{p,m}(\text{cr})\,dT - \int_{T_{fus}}^{T_{end}} C_{p,m}(\text{liq})\,dT \quad (3)$$

where Q is the energy needed to heat 1 mol of CHO from T_{start} to T_{end}. The initial T_{start} and final T_{end} temperatures lay in the temperature intervals with "normal" heat capacity. The following equations were applied to describe the heat capacity for crystalline and liquid CHO:

$$C_{p,m}(\text{cr})/\text{J·K}^{-1}\text{·mol}^{-1} = 179.94 - 0.43454(T/\text{K}) + 1.5292\cdot10^{-3}(T/\text{K})^2 \quad (4)$$

$$C_{p,m}(\text{liq})/\text{J·K}^{-1}\text{·mol}^{-1} = 60.603 + 0.58216(T/\text{K}) \quad (5)$$

The numerical coefficients were obtained from the experimental data in the intervals of (316 to 355) K and (364 to 370) K, respectively.

Thermodynamic Functions of the Condensed State. For calculation of the entropy and the enthalpy for the phases, one

Table 8. Standard Vaporization Entropies and Standard Entropy of a Gas for CHO

	$\Delta^{g}_{cr}S^{\circ}_{m}(T)$	$\Delta^{T}_{0}S^{\circ}_{m}$ (g, exptl)	$\Delta^{T}_{0}S^{\circ}_{m}$ (g, calcd)
T/K	J·K^{-1}·mol^{-1}	J·K^{-1}·mol^{-1}[a]	J·K^{-1}·mol^{-1}[b]
320.00	174.2 ± 1.4	373.5 ± 1.6	370.6
362.20	168.0 ± 1.4	393.2 ± 1.6	389.9

[a] The experimental standard entropy of CHO is a sum of sublimation entropy and standard entropy of the crystalline sample. [b] Calculated by the method of statistical thermodynamics standard entropy of ideal gas CHO.

has to extrapolate the experimental heat capacities below $T =$ 5 K. The extrapolation was performed with the use of an empirical equation[14]

$$C_p = D_3(\theta_D) + 3E(\theta_E) \quad (6)$$

where D_3 is the Debye heat capacity function for three degrees of freedom; E is the Einstein heat capacity function for one degree of freedom; and θ_D and θ_E are the corresponding characteristic temperatures. The characteristic temperature values for the crystal were found from the experimental heat capacities in the interval of (4.9 to 6.8) K to be $\theta_D = 87.6$ K and $\theta_E =$ 68.3 K. In that interval, the deviation of the calculated values from the experimental ones did not exceed 1.5 %.

The experimental heat capacities in the interval (5 to 370) K were fitted by polynomials. The smoothed values of the thermodynamic functions for CHO in the crystalline and liquid states are listed in Table 4.

Vapor Pressure. The results of vapor pressure determination by the integral Knudsen method are presented in Table 5, and the results of the transpiration method are shown in Table 6. The p^{sat} values for crystalline CHO obtained by the two methods agree within 2 %.

To evaluate the temperature dependence of vapor pressure, the Clarke and Glew[11] equation was used

$$\ln\left(\frac{p^{sat}}{p}\right) = A/(\theta/\mathrm{K}) + B[(1/\theta) - (1/T)] + C[(\theta/T) - 1 + \ln(T/\theta)] + D(\theta/2)[(T/\theta) - (\theta/T) - 2\ln(T/\theta)] \quad (7)$$

where θ is the reference temperature and p^{o} is a standard pressure 1 bar. For vapor pressure < 100 Pa, the coefficients A, B, C, and D correspond to $-\Delta^{g}_{cond}G^{\circ}_{m}(\theta)R$, $\Delta^{g}_{cond}H^{\circ}_{m}(\theta)/R$, $\Delta^{g}_{cond}C^{\circ}_{p,m}(\theta)/R$, and $\left(d\Delta^{g}_{cond}C_{p,m}(\theta)\,/\,dT\right)/R$, respectively. For higher pressures, the determination of the thermodynamic parameters becomes complicated since compressibility factors of the gas and the liquid should be taken into account.

The parameters of the Clarke and Glew equation for vapor pressure over crystalline CHO obtained by both methods are listed in Table 7 (eqs 1 and 2). The p^{sat} values obtained in this work by the integral Knudsen method agree with the results of the previous measurements[2] at $p^{sat} \leq 10$ Pa within the experimental uncertainty. At higher pressures, the deviations reach (10 to 15) %. In the present work, $\Delta^{g}_{cr}H^{\circ}_{m}$ (310 K) = 77.6 ± 1.4 kJ·mol^{-1} determined from the results of effusion experiments is 2.4 kJ·mol^{-1} lower than the previous value.[2] This deviation can be explained by the use of the constant value of the transmission probability coefficient and the absence of the undersaturation correction in the previous work.

The temperature dependence of vapor pressure for crystalline CHO was also determined in the transition region at $T <$ 305 K. As it was written above, the enthalpy and entropy values for this transition are rather small. Its effect on the temperature dependence of the vapor pressure is negligible compared with the uncertainty of the used methods. Therefore, no additional corrections to the enthalpy of sublimation concerning this transition was used.

Table 9. Relative Energies of CHO Conformers

	$I_A I_B I_C \cdot 10^{134}$	E_{tot}	ZPVE	$\Delta(E_{tot} + \mathrm{ZPVE})$
conformer	kg^3·m^6	Hartree	kJ·mol^{-1}	kJ·mol^{-1}
chair 1	8.80	−365.2782762	428.1	0.0
chair 2	9.01	−365.2668811	425.8	27.7
twist 1–1	8.84	−365.2725398	427.1	14.0
twist 1–2	8.59	−365.2620851	425.9	40.3
twist 2–1	8.99	−365.2696048	426.9	21.6
twist 2–2	8.67	−365.2584075	425.7	49.8

The joint treatment of the vapor pressure, calorimetric enthalpy of vaporization,[2] and the enthalpy of fusion was carried out. The vapor pressure data from this work, the inclined piston method,[15] and the previous p^{sat} measurements for liquid CHO[2] were used in the regression. The A, B, C, and D parameters for crystals and liquid phases were calculated by minimizing the equation $\Sigma_i((\ln(p_i^{sat}(T)/p^{sat}(\mathrm{calcd})))^2 w_i + w_i(\Delta^{g}_{cond}H_m(\mathrm{exptl}) - \Delta^{g}_{cond}H_m(\mathrm{calcd}))^2/R^2T^2 + w_i(\Delta^{1}_{cr}H_m(\mathrm{exptl}) - \Delta^{1}_{cr}H_m(\mathrm{calcd}))^2/R^2T^2_{fus} + (\ln(p^{sat}(\mathrm{cr},T_{fus})/p^{sat}(\mathrm{liq},T_{fus})))^2 w_i)$ where w_i are the statistical weights for the used methods. The θ temperatures were taken to be 316 K for crystal and 400 K for liquid (the mean temperatures of the measurements). The statistical weights were adjusted to reduce the deviation of the fitted data from the experimental ones down to the values of experimental uncertainty. Additionally, the $p^{sat}(\mathrm{cr}, T_{fus}) = p^{sat}(\mathrm{liq}, T_{fus})$ condition with the statistical weight corresponding to the experimental uncertainty of T_{fus} of ± 0.04 K was used. For crystalline CHO, the A and B coefficients of eq 7 were found from the regression, and the value of $C = -50/R$ was calculated from the difference of the ideal gas heat capacity of CHO and the heat capacity of the crystalline substance. Four parameters

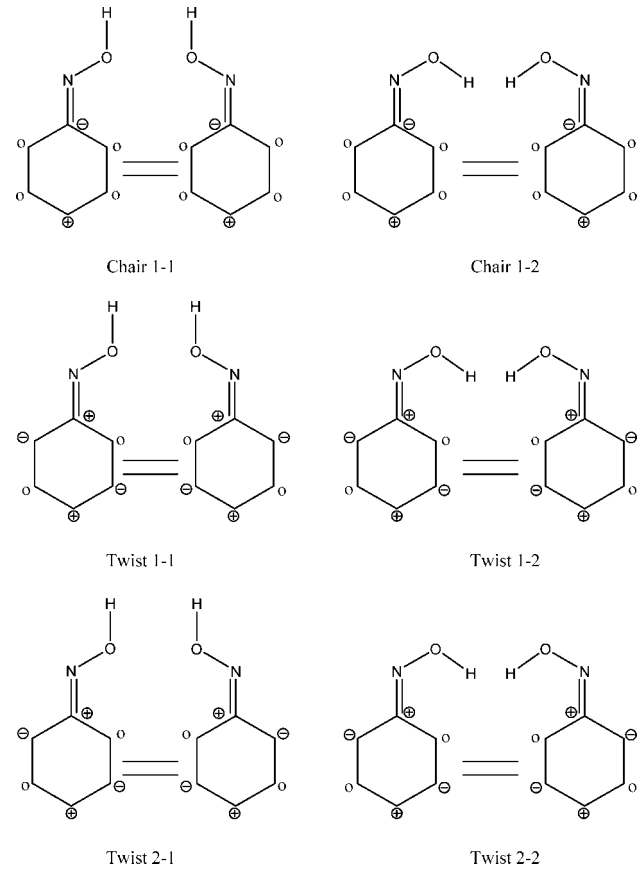

Figure 5. Conformers of the CHO Molecule.

Table 10. Experimental and Calculated Vibrational Frequencies for the Chair 1-1 Conformer[a]

ϖ_{exptl}/cm^{-1}				ϖ_{calcd}	IR intensity	Raman intensity	recommended wavenumbers
CCl_4 solution		KBr pellet		cm^{-1}	10^{13} $C^2 \cdot kg^{-1}$	10^{12} $m^4 \cdot kg^{-1}$	cm^{-1}
3606	s			3801	9.97	9.03	3646[d]
		3315	m				
3272	s	3236	s				
		3190	vs				
3120	m	3114	vs				
		3087	sh				
				3124	1.28	3.70	*2993*
2990	sh	2986	m	3109	3.53	5.64	2990
		2960	sh				
2935	vs	2935	vs	3073	9.90	6.93	2935
				3068	11.04	10.84	2935
				3049	11.98	7.71	2935
2892	sh	2898	s	3022	8.77	5.37	2892
				3020	2.63	2.22	2892
				3016	0.29	1.51	*2889*
2860	s	2858	s	3005	2.25	14.69	2860
				3002	4.26	3.65	2860
1666	m	1665	s	1731	1.41	1.34	1666
1478	sh	1482	s				
1460	sh	1460	w	1517	0.11	0.06	*1467*
				1506	2.10	0.44	1448
1448	s	1449	s	1500	0.92	0.40	1448
1437	m	1438	m	1497	1.24	0.52	1437
1431	sh	1430	sh	1489	0.80	1.02	1431
1371	w			1429	6.76	0.40	1371
1346	w	1352	m	1388	0.01	0.12	1346
		1346	w	1382	0.39	0.13	1346
1339	sh	1339	w	1371	0.36	0.14	1339
		1328	w				
1319	m	1318	m	1362	1.72	0.61	1319
				1356	0.57	0.21	1319
1270	vw	1274	vw	1305	0.17	0.39	1270
1252	m	1254	m	1283	0.80	0.48	1252
1242	w	1249	sh	1271	3.85	0.14	1242
1221	m	1226	m	1256	2.12	0.49	1221
1165	wide						
1138	m	1139	m	1163	0.74	0.16	1138
1125	vw						
1105	m	1107	m	1136	1.32	0.22	1105
1087	sh	1088	vw	1114	0.25	0.08	1087
1074	vw	1073	vw	1080	0.09	0.25	1074
1023	w	1025	m/w	1034	0.15	0.41	1023
991	s	994	vs	1002	7.16	0.25	991
962	m	963	vs				
949	s			963	13.05	0.17	949
933	w	937	vw				
922	m	924	m	941	3.91	0.09	922
897	s	901	s	903	5.50	0.11	897
857	w	858	m	875	0.26	0.01	857
839	m	841	m	842	0.64	0.26	839
		797	m	793	0.17	0.02	797
		778	m	766	0.11	0.64	778
658	m	660	m	662	0.82	0.08	658
559	m	569	m	573	2.49	0.25	559
480	w	479	w	500	5.13	0.04	*507*
460	vw			445	11.44	0.19	*454*
433	vw	434	vw	437	3.83	0.12	*446*
				392	0.48	0.10	399[b,c]
				341	0.86	0.12	356[b,c]
				306	0.13	0.03	*317*
				265	0.09	0.08	286[c]
				175	0.01	0.03	189[b,c]
				88	0.03	0.07	*96*

[a] Notes. Wavenumbers written in italics are calculated values. [b] From ref 2. [c] From ref 21. [d] Gas-phase IR-spectrum;[20] vs, is very strong, s is strong, m is middle intensity, m/w is middle weak, w is weak, vw is very weak, sh is shoulder.

were used to fit the vapor pressures over liquid CHO. The values of the coefficients are listed in Table 7 (rows 4 and 4), and the deviations of the data are shown in Figures 3 and 4.

The calorimetric value of the sublimation enthalpy, $\Delta^{g}_{cr}H^{\circ}_{m}(354\ K) = 74.0 \pm 0.3\ kJ \cdot mol^{-1}$, obtained earlier[2] and that from the fitting equation, $\Delta^{g}_{cr}H^{\circ}_{m}(354\ K) = 76.72 \pm 0.03\ kJ \cdot mol^{-1}$ deviate strongly. The older value seems to be erroneous; it was excluded from the joint regression.

Based on the results obtained in this work, the standard entropy of gaseous CHO was calculated (Table 8). The standard entropy of gaseous CHO obtained in the previous investigation[2] was $\Delta^{T}_{0}S^{\circ}_{m}(320\ K, g) = (371.5 \pm 1.0)\ J \cdot K^{-1} \cdot mol^{-1}$. The

Table 11. Thermodynamic Properties of CHO in the Ideal Gas State (M = 0.11316 kg·mol^{-1})

T/K	$\Delta_0^T S_m^\circ$ / J·K^{-1}·mol^{-1}	$C_{p,m}^\circ$ / J·K^{-1}·mol^{-1}	$\Delta_0^T H_m^\circ/T$ / J·K^{-1}·mol^{-1}	$-\Delta_0^T G_m^\circ/T$ / J·K^{-1}·mol^{-1}	$\Delta_f H_m^\circ$ / kJ·mol^{-1}	$\Delta_f G_m^\circ$ / kJ·mol^{-1}
0	0	0			35.1	−35.1
100	265.9	53.1	40.3	225.6	50.8	−4.8
200	313.9	90.9	55.9	258.0	63.4	46.3
298.15	358.3	135.7	74.6	283.7	74.4	102.5
400	405.1	185.2	96.5	308.6	83.6	164.4
500	451.2	228.7	118.7	332.6	89.8	227.2
600	496.2	264.2	140.1	356.1	93.8	291.0
700	539.1	292.4	159.9	379.2	95.8	355.3
800	579.7	314.9	177.9	401.8	96.4	420.1
900	617.9	333.3	194.2	423.7	95.8	484.3
1000	653.8	348.4	208.9	444.9	94.3	548.7

agreement between the experimental and calculated standard entropies of gaseous CHO is much better than in a previous investigation[2] (Table 2).

Theory. To calculate the thermodynamic properties of CHO in the ideal gas state, one needs to know the number of conformers formed by the CHO molecule and their relative energies. The structure of the CHO molecule is similar to the structure of the cyclohexanone molecule.[16] So, one may assume that the following conformers are formed: one "chair" conformer, three "twist" conformers, and three "bath" conformers. The quantum-chemical calculations were carried out in terms of the density functional theory at the B3LYP/6-311G(d) theory level[17,18] using the PC GAMESS 7.0 package.[19] Among the abovementioned conformers, only chair 1, twist 1, and twist 2 conformers were found to correspond to the energy minima. The relative energies of the stable CHO conformers are listed in Table 9.

The internal rotation around the N−O bond can occur in the ═N−O−H group. The relative energies between the conformers with the different −OH positions were calculated to be ca. 28 kJ·mol^{-1} (Figure 5, Table 9).

Thus, the CHO molecule possesses six chiral pairs of stable conformers (Figure 5). The chair 1 is the most stable conformer. For $T \approx 300$ K, the content of the other conformers is < 1 %.

The products of the principal moments of inertia $I_A I_B I_C$ for the conformers (Table 9) were calculated from the calculated molecular geometry.

The complete set of fundamentals for the "chair 1" conformer was compiled using the results of quantum-chemical calculations, the IR spectra of CHO in 1 % CCl_4 solution (Figure S1), in crystalline (Figure S2) and gas[20] states, and the Raman spectra in the crystalline state.[2,21] The correspondence between the experimental and the calculated values of fundamentals was found with the use of the calculated and observed absorption intensities of the Raman and IR bands. In the compilation, the experimental values of the frequencies of normal modes were preferred (Table 10).

From the quantum-chemical calculations, it was established that the change of the C═N−O−H torsion angle contributes significantly to the modes with wavenumbers of (437, 445, and 500) cm^{-1}. The calculated IR intensity of these modes is rather high (Table 10), but no high-intensity band is observed in the wavenumber range of (400 to 500) cm^{-1}. The possible cause of this fact is the absence of the CHO molecules without a hydrogen bond both in the crystal[22] and in the CCl_4 solution. Therefore, for these modes, the calculated values of the frequencies were used.

The vibrational frequencies calculated quantum mechanically are usually higher than the experimental ones. To find the vibrational frequencies not observed in the experimental spectra and to correct the calculated spectra for the minor conformers, the values of scaling factors $\chi = \varpi_{exptl}/\varpi_{calcd}$ were calculated. The experimental data for CHO and caprolactam[4] were used. For the region ($90 < \varpi < 1800$) cm^{-1}, the next empirical equation was obtained

$$\chi = (1.282 \pm 0.035) - (4.30 \pm 0.52) \cdot 10^{-2} \ln(\varpi_{calcd}/\mathrm{cm}^{-1}) \quad (8)$$

The scaling factor for the higher frequencies was found to be (0.958 ± 0.011).

The procedure of statistical thermodynamic calculations of the thermodynamic properties in the ideal gas state was described in detail elsewhere.[23] The thermodynamic properties of CHO in the ideal gas state were calculated over the interval of (100 to 1000) K (Table 11). The entropy of CHO in the ideal gas state in the interval of (320 to 362.2) K calculated by the statistical thermodynamics agrees with the experimental results within 1 % (Table 8). This deviation is significantly less than the total uncertainty of the used experimental methods.

To calculate the enthalpy of formation of gaseous CHO $\Delta_f H^\circ$(g, 298.15 K) = −(74.4 ± 2.5) kJ·mol^{-1}, the experimental enthalpy of formation for crystalline CHO $\Delta_f H^\circ$(cr, 298.15 K) = −(153.2 ± 2.5) kJ·mol^{-1} obtained from the bomb calorimetry experiments[2] and the sublimation enthalpy from this work (Table 7, eq 3) were used.

Supporting Information Available:

The IR spectra of CHO in KBr pellet and CCl_4 solution. This material is available free of charge via the Internet at http://pubs.acs.org.

Literature Cited

(1) Ren, R. X.; Zueva, L. D.; Ou, W. Formation of ϵ-caprolactam via catalytic Beckmann rearrangement using P_2O_5 in ionic liquids. *Tetrahedron Lett.* **2001**, *42*, 8441–8443.

(2) Kozyro, A. A.; Kabo, G. J.; Krouk, V. S.; Sheiman, M. S.; Yursha, I. A.; Simirsky, V. V.; Krasulin, A. P.; Sevruk, V. M.; Gogolinsky, V. I. Thermodynamic properties of cyclohexanone oxime. *J. Chem. Thermodyn.* **1992**, *24*, 883–895.

(3) Zaitsau, D. H.; Verevkin, S. P.; Paulechka, Y. U.; Kabo, G. J.; Sevruk, V. M. Comprehensive Study of Vapor Pressures and Enthalpies of Vaporization of Cyclohexyl Esters. *J. Chem. Eng. Data* **2003**, *48*, 1393–1400.

(4) Zaitsau, Dz. H.; Paulechka, Y. U.; Kabo, G. J.; Kolpikau, A. N.; Emel'yanenko, V. N.; Heintz, A.; Verevkin, S. P. Thermodynamics of the sublimation and of the vaporization of ϵ-caprolactam. *J. Chem. Eng. Data* **2006**, *51*, 130–135.

(5) Blokhin, A. V.; Kabo, G. J.; Paulechka, Y. U. Thermodynamic Properties of [C_6mim][NTf_2] in the Condensed State. *J. Chem. Eng. Data* **2006**, *51*, 1377–1388.

(6) Weiser, M. E. Atomic weights of the elements 2005 (IUPAC Technical Report). *Pure Appl. Chem.* **2006**, *78*, 2051–2066.

(7) Wahlbeck, P. G. Effusion. VII. The Failure of Isotropy of a Gas in an Effusion Cell and the Transition Region. *J. Chem. Phys.* **1971**, *55*, 1709–1715.
(8) Pappu, R. V.; Hart, R. K.; Ponder, J. W. Analysis and Application of Potential Energy Smoothing and Search Methods for Global Optimization. *J. Phys. Chem. B* **1998**, *102*, 9725–9742.
(9) Lide, D. R., Ed. *CRC Handbook of Chemistry and Physics: A Ready-Reference Book of Chemical and Physical Data*, 88th ed.; CRC Press: London, 2007–2008.
(10) Masherpa, G. Methodes de determination des tensions de vapeur a temperature elevee. *Rev. Chim. Minerale* **1966**, *3*, 153–184.
(11) Clarke, E. C. W.; Glew, D. N. Evaluation of thermodynamic functions from equilibrium constants. *Trans. Faraday Soc.* **1966**, *62*, 539–547.
(12) Verevkin, S. P. Substituent Effects on the Benzene Ring. Determination of the Intramolecular Interactions of Substituents in *tert*-Alkyl-Substituted Catechols from Thermochemical Measurements. *J. Chem. Eng. Data* **2000**, *45*, 946–952.
(13) Verevkin, S. P. Pure Component Phase Changes Liquid and Gas. In *Experimental Thermodynamics: Measurement of the thermodynamic properties of multiple phases*; Weir, R. D., De Loos, Th.W., Eds.; Elsevier: New York, 2005; Chapter 1, *Vol. 7*, pp 6–30..
(14) McCullough, J. P.; Scott, D. W. *Experimental Thermodynamics. Calorimetry of Non-reacting Systems*; Butterworth: London, 1968; Vol. I.
(15) Steele, W. V.; Chirico, R. D.; Cowell, A. B.; Knipmeyer, S. E.; Nguyen, A. Thermodynamic Properties and Ideal-Gas Enthalpies of Formation for 1,4-Diisopropylbenzene, 1,2,4,5-Tetraisopropylbenzene, Cyclohexanone Oxime, Dimethyl Malonate, Glutaric Acid, and Pimelic Acid. *J. Chem. Eng. Data* **2002**, *47*, 725–739.
(16) Burkert, U.; Alinger, N. L. Molecular Mechanics, ACS. Monograph 177, 1982, p 71.
(17) Becke, A. D. Density-functional thermochemistry. III. The role of exact exchange. *J. Chem. Phys.* **1993**, *98*, 5648–5652.
(18) Lee, C.; Yang, W.; Parr, R. G. Development of the Colle-Salvetti correlation-energy formula into a functional of the electron density. *Phys. Rev. B* **1988**, *37*, 785–789.
(19) Granovsky, A. A. http://classic.chem.msu.su/gran/gamess/index.html.
(20) http://webbook.nist.gov/cgi/cbook.cgi?ID=C105602&Units=SI&Mask=80.
(21) http://www.aist.go.jp/RIODB/SDBS/menu-e.html.
(22) Olivato, P. R.; Ribeiro, D. S.; Zukerman-Schpector, J.; Bombieri, G. Self-association and stereochemistry study of 2-methylthio-, 2-dimethylaminocyclohexanone oximes and the parent cyclohexanone oxime. *Acta Crystallogr. B* **2001**, *B57*, 705–713.
(23) Frenkel, M. L.; Kabo, G. J.; Marsh, K. N.; Roganov, G. N.; Wilhoit, R. C. *Thermodynamics of Organic Compounds in the Gas State*; TRC Data Series: College station, Texas, 1994.

Received for review September 21, 2007. Accepted December 13, 2007. The authors are grateful to the INTAS-Belarus foundation for financial support of this work (grant no. 03-50-5526).

JE700546R